Prospects for dilepton rates from lattice QCD

Anthony Francis

Helmholtz Institut Mainz, Johannes Gutenberg-Universität Mainz, D-55099 Mainz, Germany

E-mail: afrancis@uni-mainz.de

Abstract. We discuss the prospects of computing thermal dilepton rates from first principles lattice QCD. The focus lies in the determination of the meson vector-vector current spectral function to estimate the electrical conductivity, heavy quark diffusion and quarkonium dissociation. We review and compare recent results from continuum-extrapolated, quenched calculations, as well as dynamical two-flavor setups.

1. Electromagnetic spectral function in heavy-ion collisions

Heavy-ion collision experiments such as those carried out at RHIC, LHC and the future facilities at FAIR probe nuclear matter under extreme conditions, i.e. at high temperatures and/or baryon densities. Given the possible applications there has been a large effort from the phenomenological and theoretical communities to work out the properties of relevant observables in QCD, for recent reviews see [1, 2]. One of these is the spectral function of the electromagnetic current $J^{\rm em}_\mu = \frac{2}{3}\bar{u}\gamma_\mu u - \frac{1}{3}\bar{d}\gamma_\mu d - \frac{1}{3}\bar{s}\gamma_\mu s + ...$:

$$\rho_{\mu\nu}(\omega,\vec{p}) = \int d^4x\, e^{i\omega\cdot x_0 - i\vec{p}\cdot\vec{x}} \Big\langle 0 \Big| [J^{\rm em}_\mu(x), J^{\rm em}_\nu(0)] \Big| 0 \Big\rangle \quad , \tag{1}$$

in vacuum it is accessible to experiments from the R-ratio via the optical theorem

$$\frac{\sigma(e^+e^- \to \text{hadrons})}{48\pi^3\alpha(s)^2/(3s)} = \frac{R(s)}{12\pi^2} = \frac{1}{6\pi}\frac{\rho_{\mu\mu}(\omega^2)}{\omega^2} \quad . \tag{2}$$

Conversely the spectral function determines the production rate of lepton-antilepton pairs:

$$\frac{dN_{l^+l^-}}{d\omega d^3p} = \sum_{f=u,...} Q_f^2 \;\; \frac{\alpha_{\rm em}^2}{6\pi^3} \;\; \frac{\rho_{\mu\mu}(\omega,\vec{p},T)}{(\omega^2-\vec{p}^2)(e^{\omega/T}-1)} \quad . \tag{3}$$

The low frequency part of the spectral function is related to the transport properties of the medium. For example, in the high temperature phase and for light vector mesons, the spatial components give the response of the quark-gluon plasma (QGP) to electromagnetic fields and the soft emission rate of photons

$$\sigma_{\rm em}(T) = \sum_{f=u,d} Q_f^2 \;\; \frac{1}{6}\lim_{\omega\to 0}\frac{\rho_{ii}(\omega,\vec{0},T)}{\omega} \quad \text{and} \quad \lim_{\omega\to 0}\omega\frac{dR_\gamma}{d^3p} = \frac{3}{2\pi^2}\sigma_{\rm em}(T)T\alpha_{\rm em} \quad . \tag{4}$$

For heavy quark vector mesons the same limit gives the heavy quark diffusion coefficient D:

$$\frac{2T^2}{\kappa} = D = \frac{1}{6\chi_q} \lim_{\omega\to 0} \frac{\rho_{ii}(\omega, \vec{0}, T)}{\omega}, \tag{5}$$

where χ_q is the quark number susceptibility. For heavy quarkonia the spectral function around threshold of not only the vector but also the other possible channels is especially interesting, since the dissociation pattern can be used to define a QGP-thermometer [3].

The spectral function is related to Euclidean current-current correlation functions by the integral transform:

$$G_{\mu\nu}(x_0, \vec{p}) = \int_0^\infty \frac{d\omega}{2\pi}\ \rho_{\mu\nu}(\omega, \vec{p}, T)\ \frac{\cosh[\omega(\beta/2 - x_0)]}{\sinh(\omega\beta/2)}, \tag{6}$$

where $\beta = 1/T$ and we define the kernel $K(\omega, x_0, T) = \cosh[\omega(\beta/2 - x_0)]/\sinh(\omega\beta/2)$. This connection opens the possibility to study the spectral function indirectly via lattice QCD. The central question is, how well the numerically ill-posed inverse transform to obtain the spectral function can be controlled. In this talk, I review a selection of recent results from different lattice approaches to tackle this issue and the insights on the underlying physics phenomena gained in this way.

2. Meson correlation functions from lattice QCD

In lattice QCD, observables are computed on a set of gauge field configurations generated via Monte-Carlo methods and the discretized QCD action. The correlation functions of two mesonic (vector) currents at vanishing momentum is

$$G_{\mu\nu}(x_0, T) = \int d^3x \langle J_\mu(x_0, \vec{x}) J_\nu(0, \vec{0})^\dagger \rangle \quad , \tag{7}$$

whereby here $J_\mu(x) = \frac{1}{\sqrt{2}}\Big(\bar{u}(x)\gamma_\mu u(x) - \bar{d}(x)\gamma_\mu d(x)\Big)$ is the isospin current with only quark-line connected diagrams contributing[1]. In practice, computing this quantity on the lattice involves setting up an appropriate interpolating creation operator at the source $(0, \vec{0})$ and correlating it with a corresponding annihilation operator at the sink $(x_0, \vec{x})$ located within the four-volume of the background gauge-field configurations. To obtain a physically meaningful result the so-called "gauge average" has to be taken:

$$\langle J_\mu(x_0, \vec{x}) J_\nu(0, \vec{0})^\dagger \rangle = \frac{\int dU\ J_\mu(x_0, \vec{x}) J_\nu(0, \vec{0})^\dagger\ e^{S^{lat}_{QCD}[U]}}{\int dU\ e^{S^{lat}_{QCD}[U]}} \quad , \tag{8}$$

in the limit of infinitely many configurations this corresponds to computing the path integral over all possible gauge field backgrounds.

3. Spectral function reconstruction

The process of reconstructing the spectral function from lattice correlator data is made more difficult by the kernel $K(\omega, x_0, T)$. As such it highly suppresses the features of the spectral function itself and renders the correlator largely insensitive to them. For example, in [5, 6] mock data studies could show the difference in the correlator at the midpoint of the lattice between a

[1] Note, a recent estimate of the disconnected contribution [4] could show the isospin and electromagnetic correlators to be the same for distances up to $a \lesssim 1.5\,\mathrm{fm}$

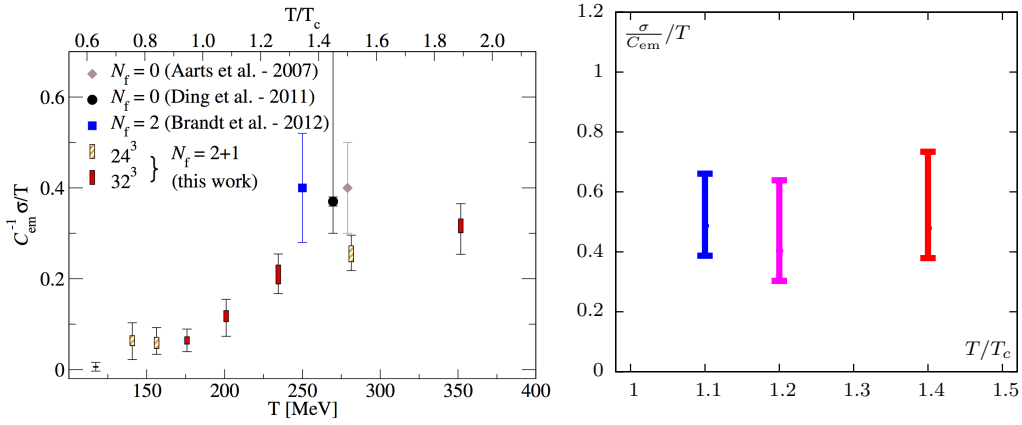

Figure 1. Left: Collected results on the electrical conductivity of the QGP across the deconfinement phase transition, provided in [8]. Right: A recent update on the electrical conductivity in the continuum limit of quenched QCD [20].

strongly peaked, i.e. bound state, and a flat, i.e. un-bound, spectral function is at the 5%-level. Taking this as an optimistic lower bound, it follows that, the lattice data has to be more precise than this value.

With precision data available, two approaches have been widely adapted to reconstruct the spectral function. The first is the "Maximum Entropy Method" (MEM) [7]. Here Bayes' theorem is invoked to determine the most probable spectral function given the data and a so-called default model. Commonplace algorithms maximize an entropy term to determine the coefficients $c(k)$ of a set of transformed basis functions $\mathcal{L}(B(k))$ to obtain an approximation of the spectral function based on the correlator data,

$$G(x_0) = \sum_k c(k)\mathcal{L}\Big(B(k,w),x_0\Big) \quad \Rightarrow \quad \rho(\omega) = \sum_k c(k)B(k,\omega) \quad , \tag{9}$$

since the inverse transformation of the basis functions is known, one thereby obtains also an estimate of the spectral function. The greatest caveat of this method is the dependence on the default model. Alternatively, instead of fixing the basis functions and determining their weights, one can define the basis functions by a set of Ansätze $F(a_k)$ for the spectral function, i.e.

$$G(x_0) = \sum_k \mathcal{L}\Big(F(a_k,\omega),x_0\Big) \quad \Rightarrow \quad \rho(\omega) = \sum_k F(a_k,\omega) \quad . \tag{10}$$

Naturally, in this case the Ansätze introduce a model-dependence and have to be justified. Generally phenomenological considerations enter the analysis at this point. Since both methods introduce a difficult to estimate degree of systematic uncertainty, due to the ill-posed nature of the inverse transformation, cross-checks using multiple approaches are mandatory.

3.1. Electrical conductivity across deconfinement and in the quenched continuum

In the case of the light vector meson spectral function and especially the electrical conductivity of the QGP a number of calculations is available, using both MEM and Ansätze for the reconstruction. In Fig. 1(left) we show a collection of results on $\sigma_{\rm em}(T)/T$ recently published[2] in [8]. Here, the first determination using staggered fermions in quenched QCD and using

[2] Note, the charge factor $\sum_f Q_f^2$ is neglected in the figure.

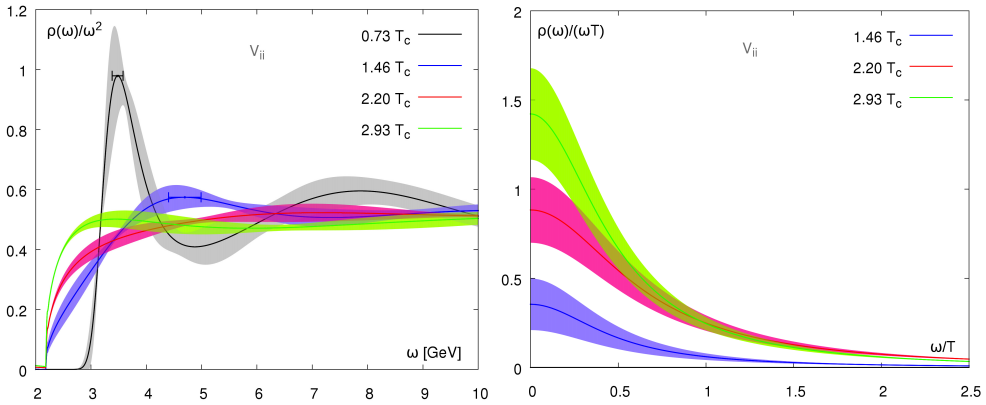

Figure 2. The vector charmonium spectral function over ω^2 (left) and ω (right) computed on large, quenched ensembles using MEM [14]. Left: The existence/non-existence of peaks is indicative of dissociation. Right: The linear intercept gives the heavy quark diffusion coefficient.

MEM for reconstruction [9] is shown in brown. Also in the quenched approximation, but using Wilson-Clover fermions, results using the Ansatz-method extrapolated to the continuum limit are given in black [10]. In the dynamical sector results obtained using ensembles with two light quark flavors of Wilson-Clover fermions and a pion mass $m_\pi \simeq 270\,\mathrm{MeV}$ are given in blue [11]. This calculation made use of the Ansatz-method and additionally incorporated QCD sum rules for further constraints on the spectral function. Finally, in yellow and red, results on anisotropic ensembles with two light and one strange quark flavor of Wilson-Clover fermions at $m_\pi \simeq 400\,\mathrm{MeV}$ are shown [8]. This study also uses MEM to reconstruct the spectral function. Recently, also the analysis using the Ansatz-method in the continuum limit of quenched QCD was updated [13, 20] to cover a temperature range of $T/T_c \in [1.1 : 1.5]$, see Fig. 1(right). Throughout, a consistent picture is emerging towards the value of σ_{em}, especially in the $T/T_c \simeq 1.5$ region. In the quenched continuum limit no clear temperature dependence can be observed, while there is a consistent drop in the dynamical case. This might be due to to different natures of the deconfinement phase transitions in these two theories and is under current investigation.

3.2. Heavy quark diffusion and quarkonium dissociation

In the case of heavy mesons, [14] used MEM to study the dissociation Fig. 2(left) and the diffusion coefficient 2(right) of charmonia on large, quenched lattices. Here, the J/Ψ was found to dissociate below $T/T_c \simeq 1.5$, while the heavy quark diffusion coefficient was found to be $\kappa/T^3 \in [4 : 7]$. A determination based on effective field theory methods [15] in the continuum limit [16] reconstructing using an Ansatz, shown in Fig. 3(left), found $\kappa/T^3 = 2.5(4)$, in line also with [17, 18, 19, 20]. This discrepancy is currently under investigation. Using NRQCD to determine the correlation functions for bottomonia [21, 22], the Υ-peak was observed for temperatures up to $T/T_c \simeq 1.9$, whereby using MEM for reconstruction, see Fig. 3(right). The emerging picture from these studies, and others not shown here e.g. [23, 24], indicates a faster dissociation of charmonia above T_c than previously thought, while bottomonia persist to larger temperatures, as expected.

4. Conclusions

In this talk I outlined the basic steps required to reconstruct spectral functions from Euclidean, lattice QCD, current-current correlation functions. The two most widely used methods for reconstruction used were also commented on. Focusing on vector mesons, the applications in heavy-ion collision physics were highlighted and a selection of studies was discussed aiming at

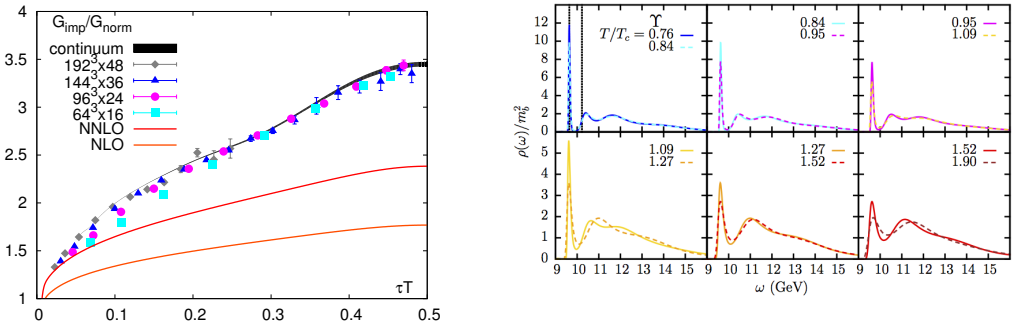

Figure 3. Left: The electric force correlator can be used to estimate heavy quark diffusion [15]. The black curve shows the result extrapolated to the continuum [16]. Right: Bottomonium spectral functions determined using NRQCD across the deconfinement phase transition [21].

providing an overview to the current status from lattice QCD. We observe an emerging agreement on the value of the electrical conductivity at large temperatures from different approaches and a fast dissociation of charmonia above the deconfinement temperature. At the same time bottomonia are seen to persist to larger temperatures. In the case of heavy quark diffusion and the electrical conductivity around the deconfinement transition work is still needed to pin down any additional systematic uncertainties. These studies are currently underway.

Acknowledgments

I wish to thank the organizers of "FAIRNESS 2014" for giving me the opportunity to present this review and for hosting such a broad and stimulating conference. Additionally I want to extend my gratitude to Gert Aarts of Swansea University for kindly sharing his results. Finally, I want to thank Harvey B. Meyer of Mainz University for looking over this draft.

References

[1] R. Rapp, *et al.*, Lect. Notes Phys. **814**, 335 (2011).
[2] R. Rapp, D. Blaschke and P. Crochet, Prog. Part. Nucl. Phys. **65**, 209 (2010) [arXiv:0807.2470 [hep-ph]].
[3] T. Matsui and H. Satz, Phys. Lett. B **178**, 416 (1986).
[4] A. Francis, V. Gülpers, B. Jäger, H. B. Meyer, G. von Hippel, H. Wittig; PoS LATTICE **2014** (2014) 128.
[5] F. Karsch, *et al.*, Nucl. Phys. A **715**, 701 (2003) [hep-ph/0209028].
[6] S. Wissel, phD-Thesis, Bielefeld University 2006.
[7] M. Asakawa, T. Hatsuda and Y. Nakahara, Prog. Part. Nucl. Phys. **46**, 459 (2001) [hep-lat/0011040].
[8] A. Amato, *et al.*, Phys. Rev. Lett. **111**, 172001 (2013) [arXiv:1307.6763 [hep-lat]].
[9] G. Aarts, *et al.*, Phys. Rev. Lett. **99**, 022002 (2007) [hep-lat/0703008 [HEP-LAT]].
[10] H.-T. Ding, *et al.*, Phys. Rev. D **83**, 034504 (2011) [arXiv:1012.4963 [hep-lat]].
[11] B. B. Brandt, A. Francis, H. B. Meyer and H. Wittig, JHEP **1303**, 100 (2013) [arXiv:1212.4200 [hep-lat]].
[12] A. Francis, *et al.*, PoS LATTICE **2013**, 453 (2013) [arXiv:1311.3759 [hep-lat]].
[13] O. Kaczmarek, *et al.*, PoS ConfinementX , 185 (2012) [arXiv:1301.7436 [hep-lat]].
[14] H. T. Ding, *et al.*, Phys. Rev. D **86**, 014509 (2012) [arXiv:1204.4945 [hep-lat]].
[15] S. Caron-Huot, M. Laine and G. D. Moore, JHEP **0904**, 053 (2009) [arXiv:0901.1195 [hep-lat]].
[16] O. Kaczmarek, arXiv:1409.3724 [hep-lat].
[17] H. B. Meyer, New J. Phys. **13**, 035008 (2011) [arXiv:1012.0234 [hep-lat]].
[18] D. Banerjee, *et al.*, Phys. Rev. D **85**, 014510 (2012) [arXiv:1109.5738 [hep-lat]].
[19] A. Francis, *et al.*, PoS LATTICE **2011**, 202 (2011) [arXiv:1109.3941 [hep-lat]].
[20] A. Francis, *et al.*, PoS LATTICE **2013**, 453 (2013) [arXiv:1311.3759 [hep-lat]].
[21] G. Aarts, *et al.*, JHEP **1111**, 103 (2011) [arXiv:1109.4496 [hep-lat]].
[22] G. Aarts, *et al.*, JHEP **1407**, 097 (2014) [arXiv:1402.6210 [hep-lat]].
[23] C. Nonaka, M. Asakawa, M. Kitazawa and Y. Kohno, J. Phys. G **38**, 124109 (2011).
[24] S. Borsanyi, *et al.*, JHEP **1404**, 132 (2014) [arXiv:1401.5940 [hep-lat]].